Numerical thermal performance study in a heat exchanger tube with inclined elliptical rings

W Sodsri[1], S Tamna[2], C Thianpong[1] and P Promvonge[1]

[1] Department of Mechanical Engineering, Faculty of Engineering, King Mongkut's Institute of Technology Ladkrabang, Bangkok 10520, Thailand
[2]Applied Mathematics and Mechanics Research Laboratory (AMM) Department of Automotive Engineering, Faculty of Engineering, TNI Bangkok, Thailand
Email: kpongjet@gmail.com

Abstract. The paper deals with a numerical study on the effect of inclined elliptical ring (IER) on heat transfer augmentation in a uniform heat-fluxed heat exchanger tube. In the present work, the 60° IER was mounted repeatedly in the tube with six different eccentricity ratios (E_R= b/a = 1, 0.9, 0.8, 0.7, 0.6 and 0.5) at a single ring-pitch ratio P_R= 1.0. Air as the test fluid flows into the tube for Reynolds number ranging from 4000 to 20,000. To find the optimum thermal performance, the effect of E_R values on the heat transfer and pressure loss is investigated. The study indicates that the use of IER can induce higher turbulent intensity imparted to the flow leading to higher heat transfer in range of about 237 to 461% above the smooth tube.

1. Introduction

Heat exchanger is a device that facilitates the exchange of heat between two different temperature fluids while keeping them from mixing with each other. Heat exchanger is widely applied in production process such as drying furnace, ventilation, air conditioning, refrigeration, electronic device, engine of machine and equipment in process industry, etc. The high performance heat exchanger is required in industry field, no matter small or large industrials take heat exchanger application in their process. At present, due to high competition and advanced development of those processes, improving their thermal performance is needed to increase efficiency. Principles used to design the device or thermal system for transfer or exchange of heat must be selected with aware of the features such as work according, laminar or turbulent flow [1], production cost, heat transfer efficacy, structure, compact size, maintenance & repair, reliability and safety. To achieve all features required, the basic key is the great allocation of resources, fuel and materials, so for allocation of resources we need to develop the capacity and potential of the heat transfer system to the best efficient, to minimize the power consumption. The design of compact size can reduce material and installation cost. Those are important that will lead to sustainable development in the future. Turbulators (turbulence promotors) are devices that can be described as static mixers. It can generate the secondary flows. Typically located inside the tubes of heat exchange equipment, turbulators can help increase the tube-side heat transfer efficiency of these units. Custom-made to fit the inside diameter of the tube, turbulators are designed to create and maintain turbulent swirl flow. There are many types of turbulators such as wire coils [2], vortex ring [3], conical rings [4], twisted tapes [5], baffles [6] and wing/ribs [7,8]. Promvonge [3] investigated the heat transfer, pressure drop and thermal performance in a round tube fitted with 30° inclined vortex rings (IVRs) with various geometry parameters such as

three relative ring width ratios and four relative ring pitch ratios. Air was employed as the test fluid for the Reynolds number from 5000 to 26,000. The IVR yields the highest TEF of about 1.4 at BR=0.1 and PR=0.5. According to the literature review above, several experimental works on heat transfer enhancement in tubes by using turbulators have been extensively reported. However, only a few numerical works on that issue have been done. Also, the application of inclined elliptical rings in a circular tube has never found in the literature. Therefore, numerical investigations for six different eccentricity ratios of 60° inclined elliptical rings (IER) are conducted to study the flow structure and thermal behaviours and to understand the mechanism of heat transfer enhancement in the tube with IER insert. In the present work, air as the test fluid enters the tube inserted with IER elements for Reynolds number ranging from 4000 to 20,000.

2. Computational model

2.1. Physical flow model

A schematic of the IER tube in this work is shown in Fig. 1. The tube has inner diameter, D = 50 mm while the IER having outer diameter of 48 mm has a ring pitch, P = D. For the elliptical ring, it has a major radius, a = 23 mm which is kept constant and a minor radius, b to be varied (see Fig.1). The inner ring shape is changed to be elliptic with eccentricity ratio, $E_R = b/a$ (= 0.5, 0.6, 0.7, 0.8, 0.9 and 1) where $E_R = 1$ means that the ring shape is circular. The heat is transferred to air through the tube wall due to different temperatures between air and tube wall. The heat transfer coefficient and pressure drop are calculated by numerical computations. The tube flow model of this work is expected to attain a periodically fully developed flow where the velocity field repeats itself from one module to another [9]. Therefore, only one module is used for the current simulation. Due to tube symmetry, only left or right half of the tube flow model is employed as computational domain as shown in Fig. 1.

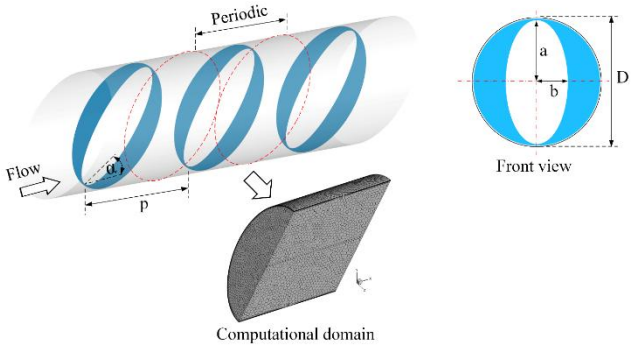

Figure 1. Tube flow model and computational domain.

2.2. Governing equations

The numerical tube flow model in the tube is developed with assumptions as follows: 1) Steady three-dimensional, turbulent and incompressible flow. 2) Constant fluid properties and 3) omitting body forces, viscous dissipation and radiation heat transfer. Based on assumptions above, the tube flow model is governed by the Reynolds averaged Navier-Stokes (RANS) equations and the energy equation. In the Cartesian tensor system these equations can be expressed as:

Continuity equation:

$$\frac{\partial}{\partial x_i}(\rho u_i) = 0 \tag{1}$$

Momentum equation:

$$\frac{\partial}{\partial x_j}\left(\rho u_i u_i\right) = -\frac{\partial p}{\partial x_i} + \frac{\partial}{\partial x_j}\left[\mu\left(\frac{\partial u_i}{\partial x_j} + \frac{\partial u_j}{\partial x_i}\right) - \rho\overline{u_i' u_j'}\right] \tag{2}$$

where ρ is fluid density, u_i is a mean component of velocity in direction x_i, p is the pressure, μ is dynamic viscosity, and u' is a fluctuating component of velocity. Repeated indices indicate summation from one to three for 3-dimensional problems.

Energy equation:

$$\frac{\partial}{\partial x_j}\left(\rho u_i T\right) = \frac{\partial}{\partial x_j}\left(\left(\Gamma + \Gamma_t\right)\frac{\partial T}{\partial x_j}\right) \tag{3}$$

Where Γ and Γ_t are molecular thermal diffusivity and turbulent thermal diffusivity, respectively and are given by

$$\Gamma = \mu / \mathrm{Pr}\text{, and } \Gamma_t = \mu_t / \mathrm{Pr}_t \tag{4}$$

The Reynolds-averaged approach to turbulence model requires that the Reynolds stresses, $-\rho\overline{u_i' u_j'}$ in (2) needs to be modeled. The Boussinesq hypothesis relates the Reynolds stresses to the mean velocity gradients as seen in (5) below:

$$-\rho\overline{u_i' u_j'} = \mu_t\left(\frac{\partial u_i}{\partial x_j} + \frac{\partial u_j}{\partial x_i}\right) - \frac{2}{3}\left(\rho k + \mu_t \frac{\partial u_i}{\partial x_i}\right)\delta_{ij} \tag{5}$$

Where k is the turbulent kinetic energy, as defined by $k = \frac{1}{2}\overline{u_i' u_i'}$, and δ_{ij} is the Kronecker delta. An advantage of the Boussinesq approach is the relatively low computational cost associated with the computation of the turbulent viscosity, μ_t given as $\mu_t = \rho C_\mu k^2/\varepsilon$. The realizable k–ε turbulence model is an example of the two-equation models that use the Boussinesq hypothesis. The steady state transport equations are expressed as:

$$\frac{\partial}{\partial x_j}\left(\rho k u_j\right) = \frac{\partial}{\partial x_j}\left[\left(\mu + \frac{\mu_t}{\sigma_k}\right)\frac{\partial k}{\partial x_j}\right] + G_k + G_b + \rho\varepsilon - Y_M + S_k \tag{6}$$

$$\begin{aligned}\frac{\partial}{\partial x_j}\left(\rho\varepsilon u_j\right) &= \frac{\partial}{\partial x_j}\left[\left(\mu + \frac{\mu_t}{\sigma_\varepsilon}\right)\frac{\partial \varepsilon}{\partial x_j}\right] + \rho C_1 S\varepsilon \\ &- \rho C_2 \frac{\varepsilon^2}{k + \sqrt{\nu\varepsilon}} + C_{1\varepsilon}\frac{3}{k} C_3 G_b + S_\varepsilon\end{aligned} \tag{7}$$

In the above equations, σ_k and σ_ε are the inverse effective Prandtl numbers for k and ε, respectively. C_1, C_2, C_3, and $C_{1\varepsilon}$ are constants. All the governing equations are discretized by the QUICK numerical scheme, coupling pressure-velocity with the SIMPLE algorithm and solved using a finite volume approach. For closure of the equations, the realizable k–ε model is used in the present study. The solutions are converged when the normalized residual values are less than 10^{-6} for all variables but less than 10^{-9} only for the energy equation. More details on boundary conditions are similar to the case in [8]. There are four parameters of interest in the present work, namely, the Reynolds number, friction factor, Nusselt number and thermal enhancement factor. The Reynolds number is defined as

$$\mathrm{Re} = \rho u_0 D/\mu \tag{8}$$

The friction factor, f is computed by pressure drop, ΔP across the length of the tube, L as

$$f = \frac{\left(\Delta P/L\right)D}{2\rho u_0^2} \tag{9}$$

The local heat transfer is measured by local Nusselt number which can be written as

$$Nu_x = h_x D / k_a \tag{10}$$

where k_a is thermal conductivity of air. The area-average Nusselt number can be obtained by

$$Nu = (1/A)\int Nu_x dA \tag{11}$$

The thermal enhancement factor (TEF) is defined as the ratio of the heat transfer coefficient of an inserted tube, Nu to that of a smooth tube, Nu_0, at an equal pumping power and given by

$$TEF = (Nu/Nu_0)/(f/f_0)^{1/3} \tag{12}$$

2.3. Grid independence

Grid independence method is tested to make sure that numerical solutions are free from grids by using four levels of grid systems performed at Re = 12,000 as shown in Fig 2. Comparing the solution of Nu obtained from four different grid levels, 90,749, 187,527, 261,275 and 385,239. It is seen that the Nu difference of the two grids between 90,749 and 187,527 is 1.021% while those between 187,527 and 261,275 and between 385,239 and 261,275 were less than 1.00%. In terms of convergence time and solution precision, the grid size of 187,527 is adopted in the current work.

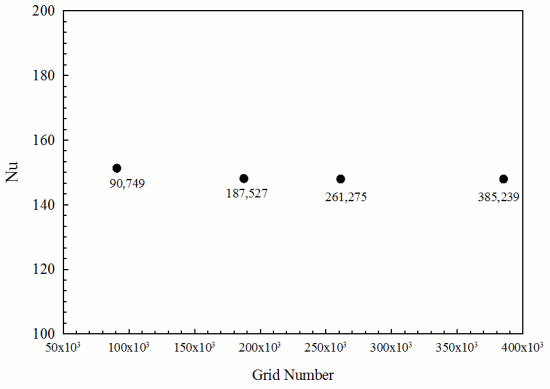

Figure 2. Grid independence test

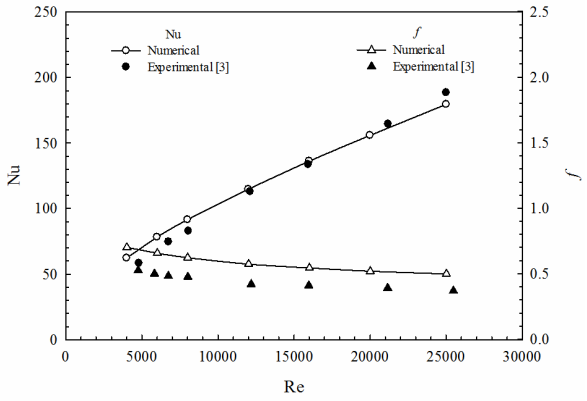

Figure 3. Validation Nu and *f* with measurements of inclined ring insert.

2.4. Model validation

It is necessary to verify the tube flow model and the method adopted in the numerical simulation. The validation of simulated Nu and *f* with Re of the tube with measurements for using 30° inclined ring insert [3] is depicted in Fig. 3. In the figure, it is found that the present numerical results and experimental data are in good agreement. The deviation of both numerical and measured data is within ± 8% for Nu and ± 18% for *f*.

3. Results and discussion

3.1. Flow structure and heat transfer

The flow structure and vortex coherent in the flow model fitted with 60° IER at E_R = 0.5, Re = 12,000 can be displayed in the form of the streamlines in transvers planes and the local Nu_x contours as shown in Fig. 4(a) and 4(b), respectively. In Fig. 4(a), the use of IER can induce two main vortices flow appearing on the left and right sides of the tube. Closer examination reveals that both are counter-rotating vortices with common-flow-down to the bottom wall. The local Nusselt number contours on the tube surface for E_R = 0.5 and Re = 12,000 are presented in Fig. 4(b). It is apparent that high Nusselt number values appear on large areas over the tube wall, especially for the area around the IER and on the bottom wall. The peaks can be observed at the impingement areas on surface close to the

IER. Also, larger regions of higher heat transfer values can be found on the bottom wall area of the tube due to common-flow-down vortices as can be seen in Fig. 4(b). This indicates that the IER enhances the heat transfer rate effectively.

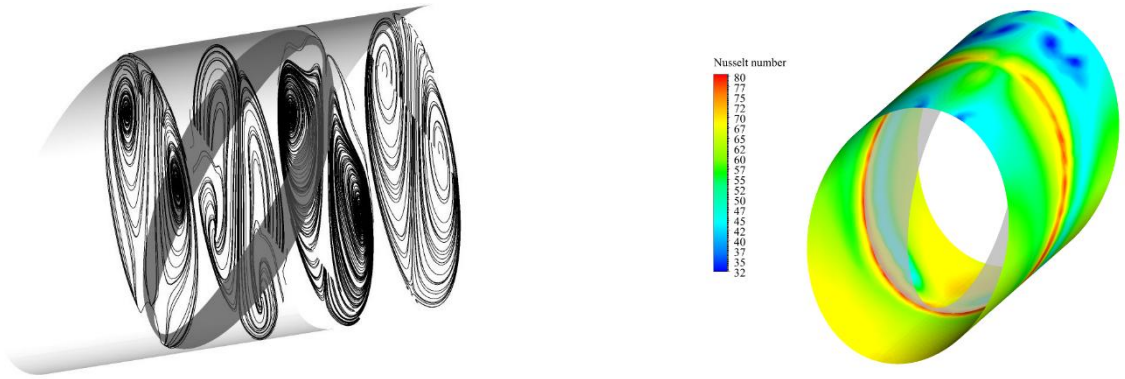

(a) (b)

Figure 4. (a) Streamlines in transverse planes and (b) local Nu_x contours for the tubes with 60° IER at E_R=0.5.

3.2. Heat transfer result

Effect of using IER turbulators with different six ER values on the heat transfer enhancement in the form of Nu/Nu_0 is depicted in Fig. 5. In the figure, Nu/Nu_0 decreases steeply with increasing Re and ER especially for Re = 4000 to 8000 but shows a gradual decrease for further Re. The maximum and minimum Nu/Nu_0 is about 6.7 and 3.6 times for E_R = 0.5, Re = 4000 and E_R = 1.0, Re = 20,000, respectively. This is because the presence of IER turbulator can interrupt the development of thermal boundary layer and increases the degree of turbulence level apart from inducing two counter-rotating vortices. The smaller E_R yields the considerable increase in the heat transfer because of higher flow blockage leading to higher vortex strength. The E_R = 0.5 provides the Nusselt number in the range of 4.7 to 6.7 times higher than the smooth tube.

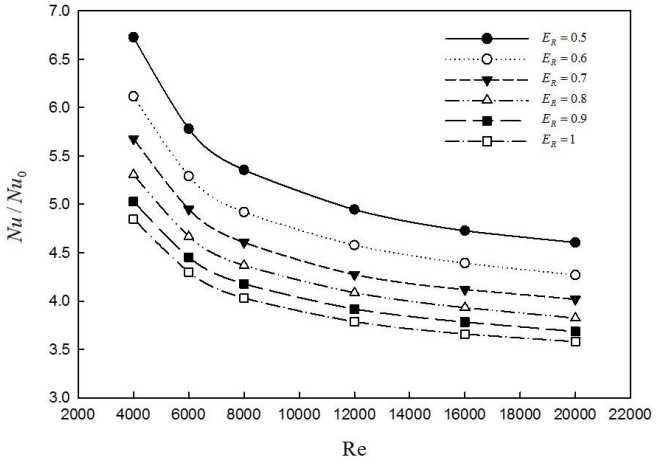

Figure 5. Nusselt number versus Reynolds number.

3.3. Friction factor result

The employ of IER insert comes with higher pressure drop in terms of friction factor. Fig. 6 displays the variation of f/f_0 with Re for various E_R values. In the figure, it is noted that f/f_0 tends to increase with the increment of Re but with decreasing E_R. The presence of IER provides the f/f_0 in the range of

36 to 130 times above the smooth tube. The f/f_0 for E_R=0.5 is around 82 – 130 times while that for E_R=0.9 is about 38 to 57 times that is nearly the same as that for circular ring (E_R=1.0). The friction losses mainly come from the dissipation of the dynamical pressure of the air due to high viscous losses near the wall, to the extra forces exerted by reversing flow and to higher friction of increasing surface area.

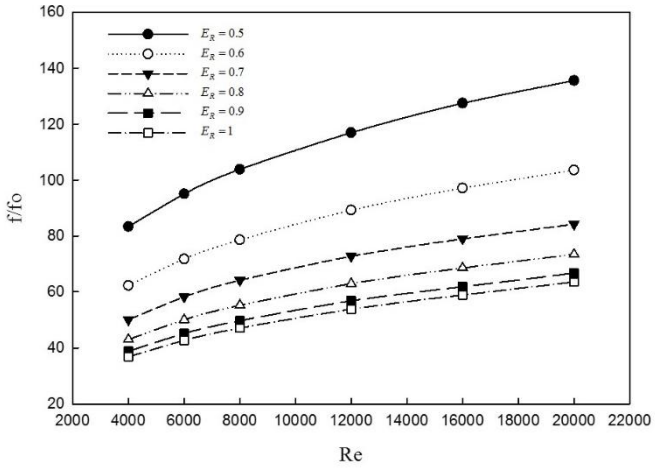

Figure 6. Friction factor against Reynolds number.

3.4. Thermal performance

Fig. 7 depicts the variation of TEF with Re for using the IER. In the figure, it is observed that TEF shows the decreasing trend with increasing Re and E_R values. The IER with E_R = 0.5, 0.6, 0.7, 0.8, 0.9 and 1 at Re=4000 provides the maximum TEF of about 1.54, 1.54, 1.54, 1.51, 1.49 and 1.46, respectively. This indicates the merit of using the IER for enhancing the heat transfer in the heat exchanger tube.

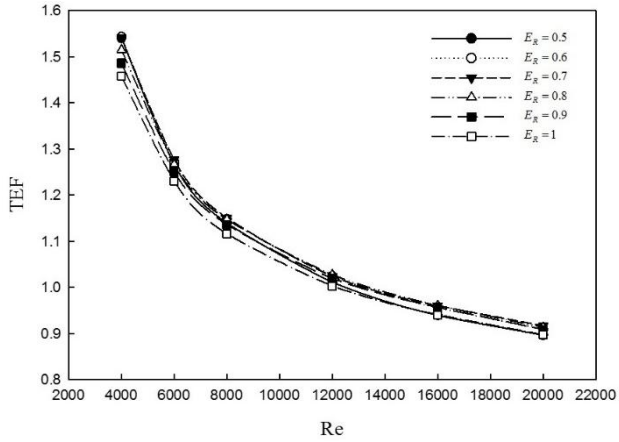

Figure 7. TEF vs Reynolds number.

4. Conclusions

Heat transfer and flow friction characteristics in a round tube with 60° inclined elliptical rings with various E_R values has been numerically investigated for the turbulent regime, Re = 4000 – 20,000 under a uniform heat-flux condition. The findings in the present study can be drawn as follows: The insertion of 60° inclined elliptical rings yields a considerable heat transfer enhancement at about 3.6 to 6.7 times above the smooth tube while the friction factor is 36 to 130 times. The Nu/Nu_0 decreases with increasing Re and E_R while f/f_0 has a similar trend except for Re that shows the reversing trend. The highest TEF of the 60° IER is found to be about 1.54 for a wide range of E_R= 0.5 – 0.7. Thus, the

application of IER insert can be considered as a promising device for augmenting heat transfer in a heat exchanger tube.

5. References

[1] Esparza D M and Rojas E S April 2011 Numerical simulations of the laminar flow in pipes with wire coil inserts *Computers & Fluids* vol 44 pp 169–77
[2] Promvonge P 2008 Thermal augmentation in circular tube with twisted tape and wire coil turbulators *Energy Conversion and Management* vol 49 pp 2949–55
[3] Promvonge P, Koolnapadol N, Pimsarn M and Thianpong C 2014 Thermal performance enhancement in a heat exchanger tube fitted with inclined vortex rings *Applied Thermal Engineering* vol 62 pp 285–92
[4] Sripattanapipat S, Tamna S, Jayranaiwachira N and Promvonge P 2016 3D Numerical Heat Transfer Investigation in a Heat Exchanger Tube with Hexagonal Conical-ring Inserts *Energy Procedia* vol 100 pp 522–5
[5] Eiamsa-ard S, Thianpong C, Eiamsa-ard P and Promvonge P 2009 Convective heat transfer in a circular tube with short-length twisted tape insert *Int. Commun. Heat Mass Transfer* vol 36 pp 365–71
[6] Skullong S, Thianpong C, Jayranaiwachira N and Promvonge P 2016 Experimental and numerical heat transfer investigation in turbulent square-duct flow through oblique horseshoe baffles *Chem. Eng. Process. Process Intensif* vol. 99 pp 58–71
[7] Skullong S, Promvonge P, Jayranaiwachira N and Thianpong C 2016 Experimental and numerical heat transfer investigation in a tubular heat exchanger with delta-wing tape inserts *Chem. Eng. Process. Process Intensif* vol 109(3) pp 164–77
[8] Promvonge P, Changcharoen W, Kwankaomeng S and Thianpong C 2011 Numerical heat transfer study of turbulent square-duct flow through inline V-shaped discrete ribs *International Communications in Heat and Mass Transfer* vol 38 pp 1392–9
[9] Patankar S V , Liu C H, and Sparrow E M 1977 Fully developed flow and heat transfer in ducts having streamwise-periodic variations of cross-sectional area *ASME, Journal of Heat Transfer* vol 99(2) pp 180–6